Journal of Materials and Environmental Science
ISSN : 2028-2508
e-ISSN : 2737-890X
CODEN : JMESCN

J. Mater. Environ. Sci., 2025, Volume 16, Issue 8, Page 1465-1480

http://www.jmaterenvironsci.com

Electrochemical and spectroscopic corrosion retardation capacity of *Urena lobata* root extract for mild steel protection in acidic medium

Enyinnaya N. P. [1*], James A. O. [1], Obi C. [1], Chukwuike V. I. [2]

[1]*Department of Pure and Industrial Chemistry, Faculty of Science, University of Port Harcourt, Port Harcourt, Nigeria.*

[2]*Department of Industrial Chemistry, Faculty of Science, David Umahi Federal University of Health Science, Uburu, Ebonyi State, Nigeria*

**Corresponding author, Email address: nwojo.enyinnaya2@gmail.com*

Received *25 May 2025,*
Revised *07 July 2025,*
Accepted *08 July 2025*

Citation*: Enyinnaya N. P., James A. O., Obi C., Chukwuike V. I. (2025) Electrochemical and spectroscopic corrosion retardation capacity of Urena lobata root extract for mild steel protection in acidic medium, J. Mater. Environ. Sci., 16(8), 1465-1480*

Abstract: This study investigates the corrosion retardation capability of root extract of *Urena lobata* (REUL) on mild steel in 0.5 M H_2SO_4 solution by electrochemical and spectroscopic methods. Potentiodynamic polarization (PDP) showed that the maximum shift in corrosion potential is $\pm$ **19 mV** indicating physical adsorption mechanism and that REUL is a mixed-type inhibitor reducing both anodic and cathodic corrosion reactions. Electrochemical Impedance Spectroscopy (EIS) results demonstrated that REUL functions by forming a protective layer on the mild steel surface, with charge transfer resistance (R_{ct}) increasing proportionally with extract concentration. The Capacitive double layer (C_{dl}) values decrease with increase in REUL inhibitor concentration from 9.3 µF cm^{-2} for blank to 5.1 µF cm^{-2} for 1.0g/L REUL resulting in protection of the metal from the corrosion effect of the acidic environment. Gas Chromatography-Mass Spectrometry (GS-MS) showed the presence of two compounds cis-vaccenic acid (43.51%) and hexadecanoic acid (56.49%). The adsorption inhibition process is spontaneous and followed Langmuir Isotherm with correlation coefficient of 0.998 and 0.989 for PDP and EIS respectively.

Keywords: *Urena lobata;Root extract; Corrosion retardation; Electrochemical study;Adsorption*

1. Introduction

Metals are obtained by extracting them from their raw forms, such as ores, through chemical reduction. In their pure forms, they are less stable but have wide applications in construction, technological, and industrial processes (Harvey *et al*., 2022; Enyinnaya *et al*., 2024). However, when exposed to different physical, biological, chemical, and biochemical environment, metals and their alloys undergo various changes and deterioration due to corrosion (Saha and Kang, 2022). Corrosion is an irreversible damage to a metal surface, resulting in the conversion of the metal into a more chemically stable form (Zomorodian *et al*., 2015). Among others, the use of inhibitors is one of the most common methods of corrosion protection in metals. A corrosion inhibitor is a substance that reduces the corrosion rate of a metal surface exposed to a corrosive environment by its chemical activity, thus extending the service life of metallic components (Bouklah *et al*., 2004; Azzaoui *et al*., 2017; Arrousse *et al*., 2021; Song *et al*., 2022). Various plant materials that have been utilized as corrosion inhibitors have been shown to

contain bioactive components, which enhance their inhibitory properties (Song *et al*., 2022; Elmsellem *et al*., 2014). The *Urena lobata* plant is commonly used as a traditional medicinal plant in Africa, India, and China, with its leaves and roots being most frequently employed (Gao *et al*., 2015). The juice of the leaves or roots is widely used to treat bowel complaints, including colic, stomachache, diarrhea, dysentery, gonorrhea, and persistent fever from malaria (Islam *et al*., 2017). Roots of most medicinal plants like *Salvadora persica* (Jasim, 2015), dandelion (Zbulj, 2022), *Biebersteinia multifida* (Khayatkashani, 2022), Rheum ribes (Kaya *et al*., 2023), *Inula viscosa* (Adil Mahraz *et al*., 2024), *Polygonum cuspidatum* (Thakur *et al*., 2024), etc have been successively employed as corrosion inhibition of metals in harsh environments.

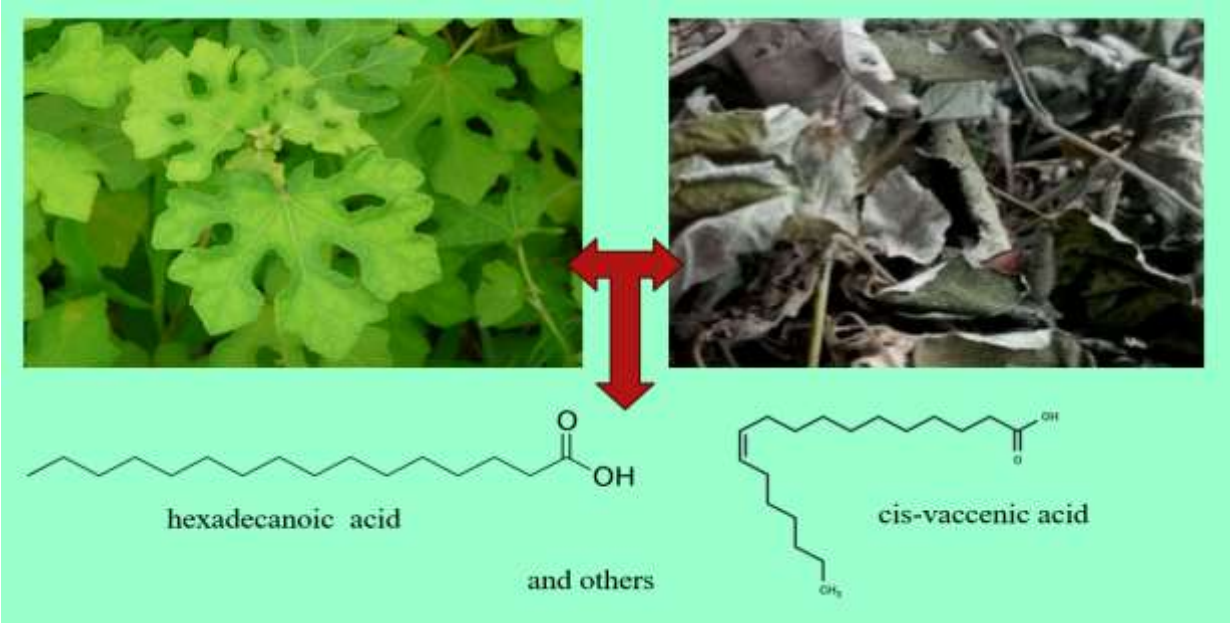

Urena lobata leaves

Although the leaves and barks of this plant, Urena lobata, have been used for medicinal purposes, no work has been done on the corrosion inhibition of its root on metals. This research aimed to spectroscopically identify the bioactive components and electrochemically evaluate the corrosion retardation ability of *Urena lobata* root extract on mild steel.

2. Methodology

2.1 Materials Collection and Preparation

Fresh *Urena lobata* roots were obtained from Farms in Aluu, Port Harcourt, Nigeria. The roots were washed under running tap, dried to constant weight under shade and ground into fine powder. The stock solution of root extract was prepared by soaking 500 g of dry root powder in 1000 g of methanol for 72 hours. The resulting solution was filtered thrice and a dark brown filtrate was obtained. The filtrate was concentrated using a rotary evaporator to obtain the methanolic root extract of Urena lobata (REUL), which was used as the inhibitor in this study. Desired concentrations of the inhibitor's solutions were prepared by measuring an accurate amount of the inhibitor and diluting with an appropriate amount of 0.5 M H_2SO_4. The mild steel sheet for this study was obtained from the Metal section of Mile 3 Market, Port Harcourt, Nigeria. The sheet was 1.5 mm in thickness and was

mechanically pressed and cut into 2 cm x 3 cm coupons. These coupons were used as cut without further polishing. The coupons were degreased in ethanol, dried in acetone, and stored in moisture-free desiccators before their use in corrosion studies.

2.2 Electrochemical Techniques

A CH electrochemical analyzer Model 604D was used to record the Tafel polarization curve and the Nyquist impedance curve. The coupons were sealed with epoxy resin in such a way that only 1cm^2 surfaces were left uncovered. The exposed surface was degreased in acetone, rinsed with distilled water, and dried in warm air. The electrochemical linear polarization experiments were conducted at a temperature of 303 K using 100 mL of test solution in a conventional three-electrode cell voltammeter. The mild steel coupons were used as working electrodes, a platinum (Pt) electrode, and a saturated calomel electrode (SCE), which served as auxiliary and reference electrodes, respectively. Before the Linear Polarization experiment, the electrode was allowed to corrode freely, and its open-circuit potential (OCP) was recorded as a function of time up to 30 min. The Tafel polarization curves were recorded by scanning the electrode potential from - 800 mV to 300 mV vs (SCE) with a scanning rate of 1 mV/s. The linear Tafel segments of the anodic and cathodic curves were extrapolated to corrosion potential to obtain the corrosion current densities (I_{corr}). The % IE was obtained from the equation below:

$$\%\,\mathbf{I.E} = \left[\frac{\mathbf{I_{corr(0)} - I_{Corr(i)}}}{\mathbf{I_{Corr(0)}}}\ \mathbf{x\ 100\%}\right] \qquad 1$$

Where $I_{corr(0)}$ is the corrosion current density of metal without inhibitor and $I_{corr(i)}$ is the corrosion current density of metal with inhibitor.

AC impedance spectra were recorded in the same instrument used for polarization study using a three-electrode cell assembly. The real part and imaginary part of the cell impedance were measured in ohms for various frequencies 100,000 to 0.1 Hz at amplitude of 10 mV and a scan rate of 10 points per decade. The charge transfer resistance values (R_{ct}) were calculated from the difference in impedance at Lower and higher frequencies (Momoh-Yahaya *et al*., 2012). The % IE was calculated from the charge transfer resistance (R_{ct}) values by using the equation:

$$\%\mathbf{I.E} = \left[\frac{\boldsymbol{R_{ct\,(i)} - R_{ct\,(0)}}}{\boldsymbol{R_{ct\,(i)}}}\ \mathbf{x\ 100\%}\right] \qquad 2$$

Where $R_{ct(0)}$ is the charge transfer resistance of the metal without inhibitor and $R_{ct(i)}$ is the charge transfer resistance of the metal with inhibitor.

2.3 REUL Inhibitor Characterization

2.3.1 UV-visible spectrophotometry

Uv-visible spectrophotometric analysis was conducted on the REUL extract using a UV-visible spectrophotometer (Shimadzu Model 240) with a slit width of 2 nm, using a 10-mm cell at room temperature.

2.3.2 Gas Chromatography – Mass Spectrophotometry (GC-MS)

This analysis was performed on the REUL using GC model: 7890A Agilent Technologies and MS model: 5975C Agilent Technologies coupled with a HP-5 capillary fused silica column (30 m x320 µm x 0.25 µm). The temperature was programmed as follows: the initial temperature was 60°C (isothermal for 4 minutes), and the final temperature was 310°C (isothermal for 5 minutes). Other operating conditions were as follows: carrier gas, helium (99.999%); pressure, 3.1325 psi; flow rate, 1.626 ml/min; and average velocity, 46.699 cm/s.

3. Results and Discussion

3.1 Potentiodynamic Polarization Studies

The polarization curves shown in **Figure 1** and the associated parameters in **Table 1** provide insights into the corrosion inhibition ability of REUL on mild steel in 0.5 M H_2SO_4. From the polarization parameter Table in **Table 1**, it is evident that the addition of REUL significantly reduces the corrosion current density (I_{corr}) compared to the blank, thereby indicating the effectiveness of the inhibition corrosion process. The reduction in I_{corr} demonstrates the protection action of REUL due to its adsorption onto the mild steel surface, thereby forming a barrier that minimizes direct acid-mild steel interaction.

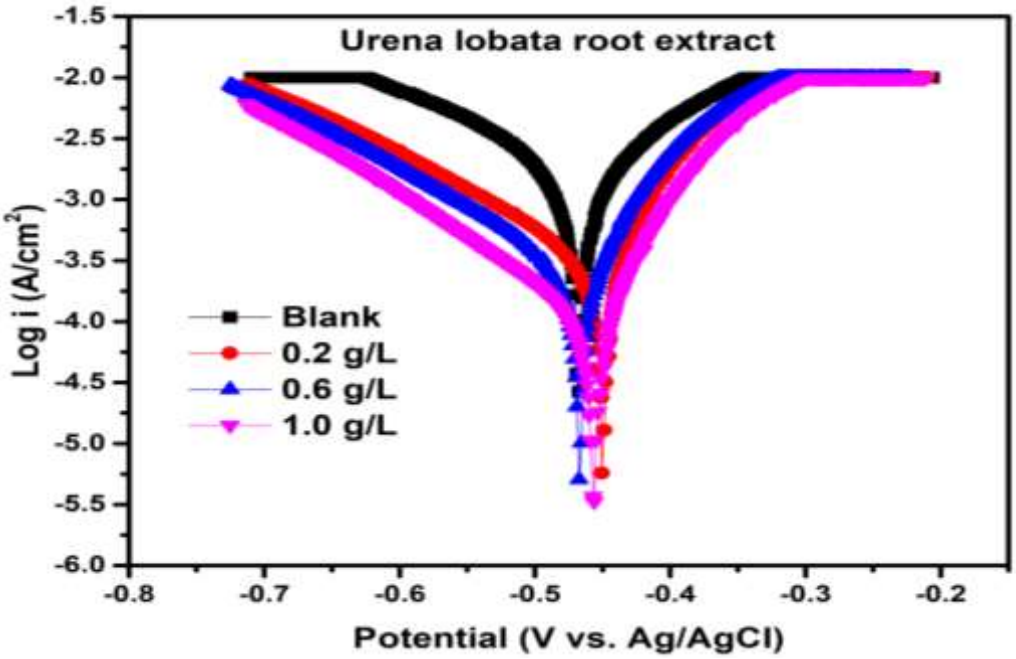

Figure 1: Potentiodynamic polarization curves for mild steel in the absence and presence of different concentrations of REUL

The anodic Tafel slope ($\boldsymbol{\beta}_a$) shows slight variation with rise in REUL concentration from 64.7 mV/Dec for blank to 54.7 mV/Dec at 1.0 g/L, indicating that the anodic metal dissolution reaction is influenced to a lesser extent. The cathodic Tafel slope ($\boldsymbol{\beta}_c$) decreases significantly with an increase in REUL concentration from 67.8mV/Dec for the blank to 101.6 mV/Dec at 1.0 g/L. This suggests that REUL predominantly affects the cathodic reaction. Thus, implying that REUL acts as a mixed–type inhibitor that is predominantly cathodic type inhibitor ($\boldsymbol{\beta}_c > \boldsymbol{\beta}_a$) (Fouda *et al.*, 2022). The corrosion potential (E_{corr}) for blank is -467.1 mV/SCE, which decreases to -448.1 mV/SCE at the highest REUL

concentration of 1 g/L at 303 K. This corresponds to a substantial increase in inhibition efficiency of 84%. At 323 K, the corrosion potential (E_{corr}) for blank is -453.8 mV/SCE, which decreases to -443.7 mV/SCE at the highest REUL concentration of 1.0 g/L with an increase in inhibition efficiency of 76.7%.

Table 1: Potentiodynamic polarization parameters for mild steel in 0.5 M H_2SO_4 solution in the presence and absence of the REUL.

Temperature K	Concentration g/L	E_{corr} mV/SCE	I_{corr} μAcm^{-2}	β_a $mVdec^{-1}$	β_c $mVdec^{-1}$	IE %
303	0.0	-467.1	594.0	64.7	67.8	-
	0.2	-463.8	243.7	59.9	139.3	59
	0.6	-456.1	163.8	56.6	133.2	72
	1.0	-448.1	97.3	54.7	101.6	84
323	0.0	-453.8	612.3	58.2	62.5	-
	0.2	-451.3	281.0	53.8	118.8	54.1
	0.6	-447.5	206.3	51.3	107.3	66.3
	1.0	-443.7	142.6	48.2	98.2	76.7

The maximum E_{corr} shift in the presence of REUL is $\pm$19 mV, which is less than $\pm$85 mV, implying that the inhibition mechanism is dominated by physical adsorption where weak van der Waals forces and hydrogen bonding play a significant role (Diki *et al.*, 2018; Jisha *et al.*, 2019; Azgaou *et al.*, 2022). However, the partial modification of both $\boldsymbol{\beta}_a$ and $\boldsymbol{\beta}_c$ suggests that some degree of chemical interaction between the REUL molecule and the mild steel surface may also occur.

3.2 Electrochemical Impedance Spectroscopy (EIS) Studies

Nyquist plots (Electrochemical Impedance Spectroscopy curves) for corrosion inhibition of mild steel in the absence and presence of different concentrations of REUL are shown in Figure 2. The Nyquist plots for the corrosion of mild steel in 0.5M H_2SO_4 in the absence and presence of REUL as depicted in **Figure 2a,** exhibit a single semicircular capacitive loop, which did not change after addition of REUL. This indicates that the mechanism of the corrosion process is under charge transfer of solution/metal interface and the dissolution mechanism did not change after addition of REUL inhibitor (Chetouani *et al.*, 2004; Idouhli *et al.*, 2018). In addition, it can be seen that the semicircular diameter of the Nyquist plots increases with rise in REUL concentration. This behaviour indicates that REUL were adsorbed onto the mild steel active sites thereby forming a thin protective inhibition layer which increase with increase in concentration of REUL (Sanaei *et al.*, 2019; Lahmady *et al.*, 2023; Udom *et al.*, 2025).

Bode plots Figure 2b showed that the addition of REUL inhibitor increases the impedance modulus at low frequencies while the impedance modulus values in the blank solution are relatively lower. This increase indicates that REUL enhances the mild steel surface resistance against corrosive attacks in the acidic phase (Hadisaputra *et al.*, 2025). This is because when REUL concentration is increased; a more protective coating layer is formed, which reduces the surface wettability, thereby inhibiting the access of H^+ and SO_4^{2-} to the mild steel surface. Thus, enhancing the electrochemical stability of mild steel in an acidic environment.

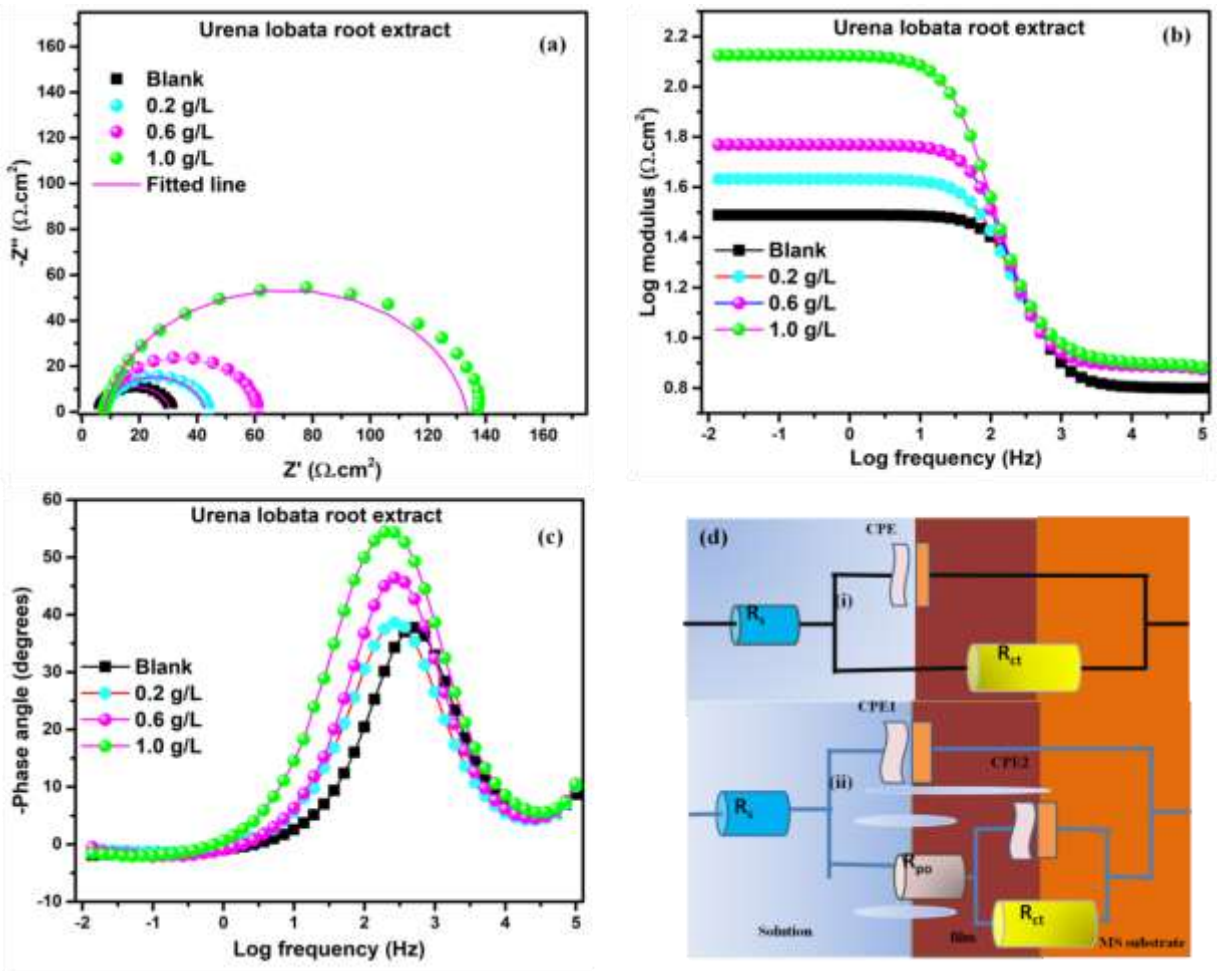

Figure 2: EIS curves for mild steel in absence and presence of different concentration of REUL

Table 2: Electrochemical Impedance parameters (EIS) for mild steel in 0.5 M H_2SO_4 solution in the presence and absence of REUL

Concentration (g/L)	R_s (Ω cm^2)	R_{po} (Ω cm^2)	Q x 10^{-5} ($\mu\Omega^{-1}s^n cm^{-2}$)	n1	R_{ct} (Ω cm^2)	C_{dl} x 10^{-5} (μFcm^{-2})	I.E %
0.0	6.3	-	50.0	0.81	14.53	9.3	-
0.2	5.8	7.8	4.5	0.83	35.09	7.1	59
0.6	6.3	7.7	3.9	0.98	50.99	5.5	72
1.0	6.3	7.8	3.2	0.99	125.80	5.1	88

Figure 2c shows the plots of Phase angle against log frequency. At -1.9 Hz, the phase angles for the inhibited and blank solutions were approximately 0°. The phase angle increases with frequency with the most significant positive peaks observed at 2.9 Hz for blank (38°), 0.2 g/L (40°), 0.6 g/L (48°) and 1.0 g/L (55°). The phase angle, which shifted toward more positive values when the amount of REUL increased, signifies a higher adsorption of the REUL inhibitor molecule onto the mild steel surface at increasing concentration (de Britto Policarpi *et al.*, 2020; Ouestlati *et al.*, 2025). The larger peak heights observed at higher inhibitor concentrations indicate a strong capacitance response (Pal and Das, 2022).

The fitting of the Nyquist plot to the selected circuit is shown in Figure 2d. To activate the impedance data, a single-layer circuit was used for the blank system and a double-layer circuit for the inhibited system to model the impedance spectra.

The Capacitive double layer (C_{dl}) values (shown in Table 2) decrease with increase in REUL inhibitor concentration. The reduction in C_{dl} value from 9.3 µF cm^{-2} for blank to 5.1 µF cm^{-2} for 1.0g/L REUL suggests that water molecules at the metal/solution interface are gradually replaced by REUL molecules, leading to a decrease in dielectric constant and an increase in electrical double-layer thickness. This results in protection of the metal from the corrosion effect of the acidic environment (Fouda *et al*., 2022; Udom *et al*., 2025).

Table 2 shows that the Charge transfer resistance (R_{ct}) values increase significantly with an increase in the concentration of REUL inhibitor. The R_{ct} values increase from 14.53 Ω cm^2 for blank to 35.09 Ω cm^2, 50.99 Ω cm^2, and 125.80 Ω cm2 for 0.2 g/L, 0.6g/L, and 1.0 g/L, respectively. This increase in R_{ct} values indicates a reduced rate of the charge transfer process, confirming the formation of a protective layer on the mild steel surface.

From Table 2, it can also be observed that the values of n1 for inhibitor samples are higher than those of the blank sample (0.81). This observation suggests that the presence of an inhibitor in the corrosive acidic environment reduces the irregularity of the mild steel surface (Adil Mahraz *et al*., 2024). This reduction was due to the formation of a protective organic film on the mild steel surface. Moreover, the n1 values (0.81–0.99) are close to 1, indicating that the interface is capacitive (Ismail *et al*., 2022). The above findings signify that REUL molecules adsorb onto the mild steel surface, forming a protective barrier film that impedes mass and charge transfer processes. The increase in REUL concentration, which enhances inhibition efficiency (%I.E.), is attributed to an increase in surface coverage by the extract, thereby blocking the active corrosion sites on the mild steel surface.

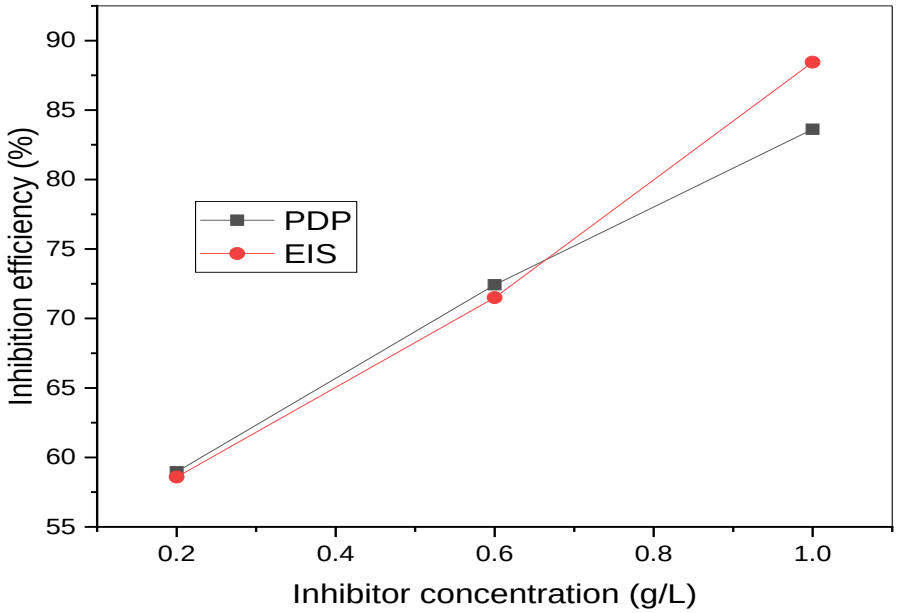

Figure 3: Variation of inhibition efficiency of REUL for corrosion of MS in 0.5 M H_2SO_4 with different inhibitor concentration

3.3 Temperature Effect

Temperature effect on the activation enthalpy (ΔH_a), activation entropy (ΔS_a), activation energy (E_a) and corrosion current density (i_{corr}) of REUL on mild steel corrosion can be examined using the Transition state and Arrhenius equations as shown in equations (3) and (4) below:

$$\log \frac{i_{corr}}{T} = -\frac{\Delta H_a}{2.303R}\left(\frac{1}{T}\right) + \left[\frac{\Delta S_a}{2.303R} + \log\left(\frac{R}{Nh}\right)\right] \quad (3)$$

$$\log i_{corr} = -\frac{Ea}{2.303R}\left(\frac{1}{T}\right) + \log A \quad (4)$$

Where, R is the universal gas constant, N is the Avogadro's number, h is the Planck's constant and T is the temperature. A plot of $\log \frac{i_{corr}}{T}$ against $\frac{1}{T}$ (Figure 4) gave straight line with slope and intercept as $\frac{\Delta H_a}{2.303R}$ and $\left[\frac{\Delta S_a}{2.303R} + \log\left(\frac{R}{Nh}\right)\right]$ respectively; from where ΔH_a and ΔS_a can be calculated. Similarly, a plot of $\log i_{corr}$ against $\frac{1}{T}$ (Figure 5) gave straight line with slope and intercept as $\frac{E_a}{2.303R}$ and $\log A$; from where E_a can be calculated. The values of E_a, ΔH_a and ΔS_a are shown in Table 3.

Table 3: Thermodynamic parameters of REUL adsorption on the mild steel 303 K and 323 K. temperatures

Concentration (g/L)	ΔH_a (kJ/mol)	ΔS_a (J/mol^{-1}K^{-1})	E_a (kJ/mol)	$E_a - \Delta H_a$ (kJ/mol)
Blank	-1.361	`-196.474	1.239	2.60
0.2	3.201	-188.829	5.800	2.60
0.6	6.795	-180.267	9.405	2.61
1.0	12.981	-164.190	15.581	2.60

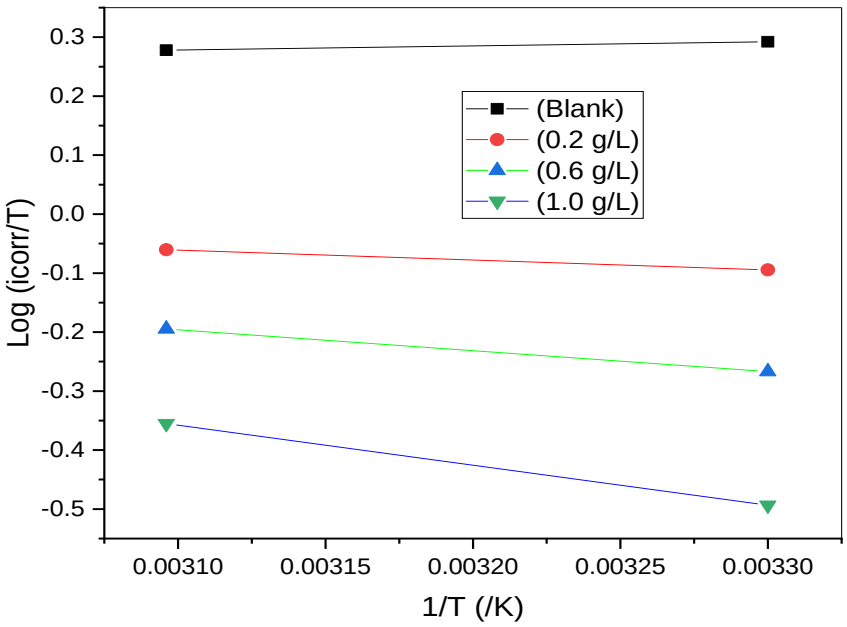

Figure 4: Transition state plots in the presence and absence of different concentrations of REUL on mild steel inhibition

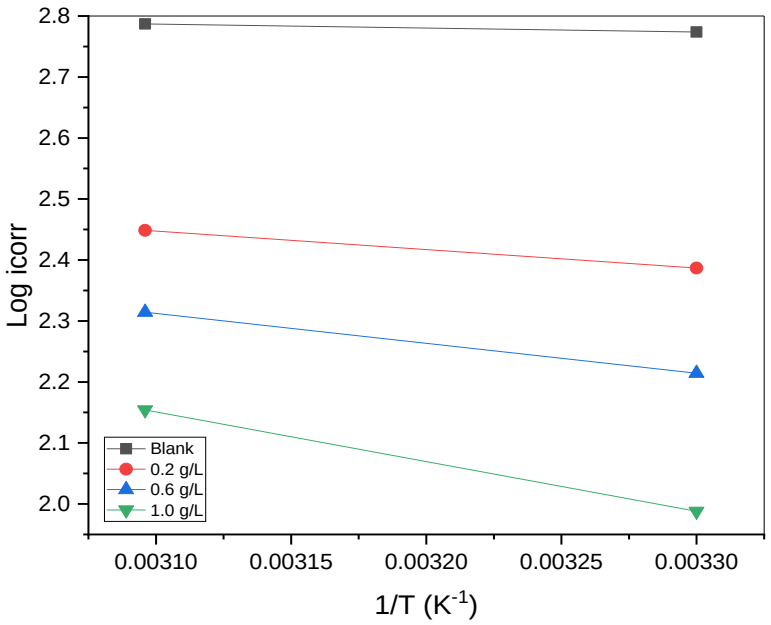

Figure 5: Arrhenius plots in the presence and absence of different concentrations of REUL on mild steel inhibition

As can be seen from Table 3, addition of REUL in 0.5 M H_2SO_4 increased the value of $\mathbf{E_a}$, indicating that the phytochemicals in REUL adsorbed onto the mild steel through van der Waals forces leading to physical adsorption (Fouda *et al.*, 2021; Enyinnaya *et al.*, 2022). The E_a values greater than 80 kJ/mol represent chemical adsorption while that below 80 kJ/mol represent physical adsorption (Enyinnaya *et al.*, 2021). Because the maximum E_a value obtained in the presence REUL (15.581kJ/mol) is less than 80 kJ/mol, it represents physical adsorption mechanism. Moreso, addition of REUL leads to increase $\mathbf{\Delta S_a}$ resulting in increased disorderliness from reactants to the activated complex (Karra *et al.*, 2025). Finally, increase in concentration of REUL led to an increase in the positive values of ΔH_a. That is, the reaction is endothermic (Shathani *et al.*, 2025). Since the values of ΔH_a are well below 40 kJ/mol, it confirms that the adsorption of REUL onto the mild steel surface is mainly by physiosorption (Enyinnaya *et al.*, 2021; Shathani *et al.*, 2025).

3.4 Ultraviolet – Visable (UV-Vis) Spectroscopy

Absorption of radiation in the UV region is made possible by the presence of loosely bound electrons, such as are found in non-bonding and pi-molecular orbitals. Electron excitation occurs between Highest Occupied Molecular Orbital (HOMO) of the ground state and Lowest Unoccupied Molecular Orbital (LUMO) of the excited state when an electron absorbs UV radiation. The appearance of absorption peaks in the region from 200 – 400 nm indicated the presence of heteroatoms like O, S and N and unsaturated bonds (Njoku *et al.*, 2013). Analysis of REUL inhibitor spectrum in Figure 6a showed that there was excitation of an electron from a non-bonding (n) or pi-bonding molecular orbital to a much lower unoccupied pi*- antibonding molecular orbital, as can be seen with the appearance of three peaks (peak 1, 2, and 3).

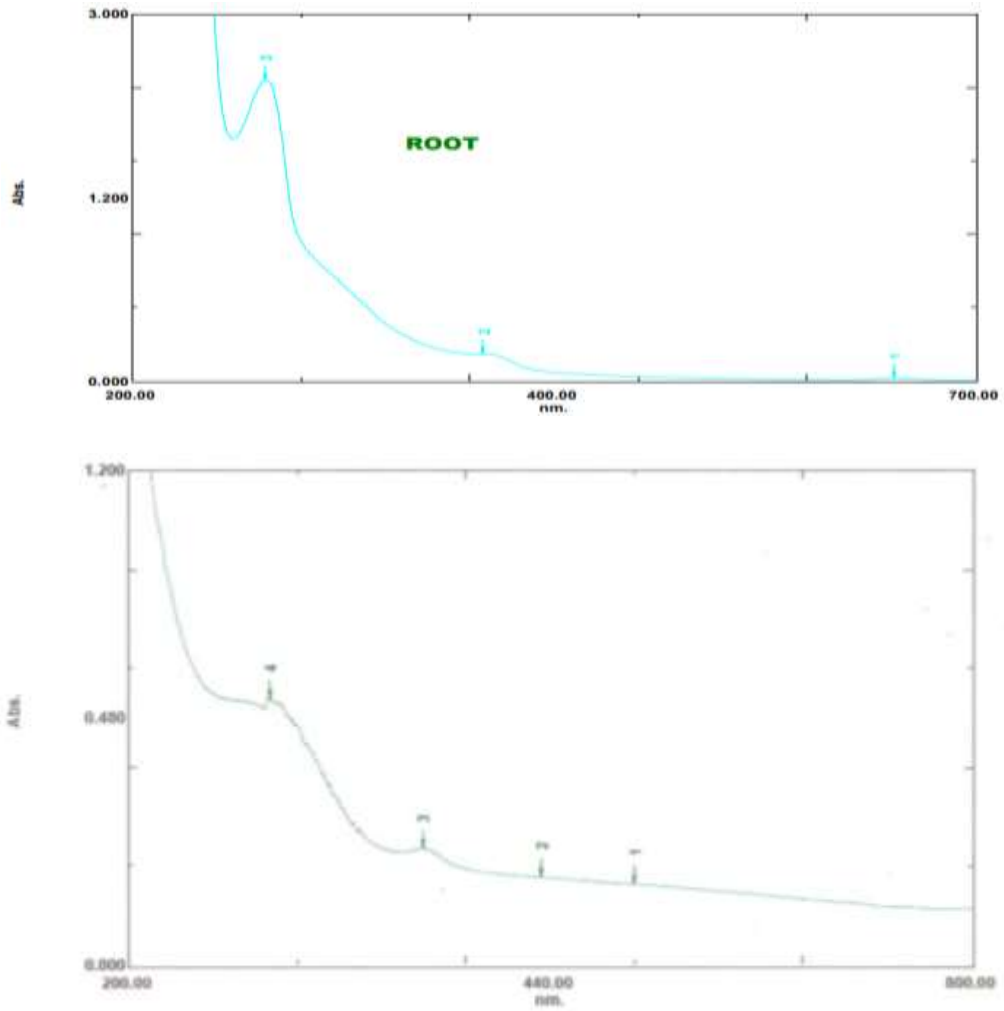

Figure 6: Uv-Visible Spectroscopy of REUL inhibitor (a) before and (b) after immersion

After immersion (Figure 6b), the absorption peak intensity decreases due to a reduction in the concentration of active phytochemicals in REUL, resulting from their adsorption onto the mild steel surface (Rahmouni *et al.*, 2025). Additionally, changes in the shape of the UV-spectra before and after immersion, suggest the formation of complexes between the REUL inhibitor and mild steel (Di Meo *et al.*, 2022). Due to inherent difficulties in assigning absorption peaks to specific constituents, UV-Visible results are often supplemented with GC-MS analysis to facilitate proper characterization and identification of constituent compounds.

3.5 Gas Chromatography – Mass Spectrophotometry (GC-MS)

The GC-MS result of REUL revealed the presence of n- Hexadecanoic acid and Cis-vaccenic acid with unsaturated bond and heteroatoms as shown in Figure 7 and Table 4. These compounds enhance the release of electrons from REUL to the mild steel surface thereby resulting in corrosion inhibition of mild steel. Literature indicated that the methanol extract revealed 47 bioactive compounds especially those having the highest abundance, n-hexadecanoic acid (26.65%) and (9.11%), dodecanoic acid (6.89%), 1-docosene (6.06%), erucic acid (4.09%) (Keke *et al.*, 2023). These phytocompounds and many others present in the leaf have been reported to possess multiple therapeutic activities (Singare *et al.*, 2022).

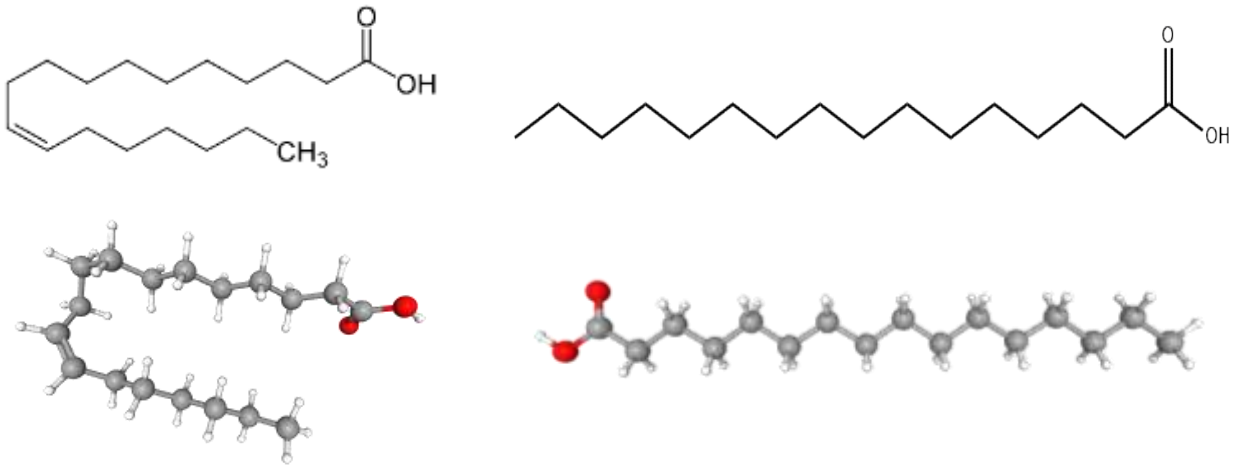

Cis–vaccenic acid

n-Hexadecanoic acid or Palmitic acid

Figure 7: Chemical structures of compounds identified in the GC-MS of REUL

Table 4: Suggested compounds identified from GC-MS of REUL

S/No	Name	Molecular Formula	Molar mass (g/mol)	Retention time (s)	% Peak area
1.	n- Hexadecanoic acid	$C_{16}H_{32}O_2$	256	13.718	56.49
2.	Cis – Vaccenic acid	$C_{18}H_{34}O_2$	282	16.143	43.51

3.6 Adsorption Isotherm

Adsorption of REUL on mild steel surface was analysed using Langmuir Adsorption Isotherm. The Langmuir Isotherm plots and the parameters obtained from the plot for PDP and EIS are shown in **Figure 8** and **Table 5** respectively. From **Table 5**, the adsorption-inhibition processes followed physical adsorption mechanism with Langmuir R-squared values of 0.998 and 0.989 for PDP and EIS respectively. The values of Gibb's Free energy of adsorption process (ΔG_{ads}) for PDP and EIS are -9.633 kJ/mol and -9.721 kJ/mol respectively. Since these values are less than 40 kJ/mol; it showed that the adsorption process is physical adsorption and spontaneous (Nzeneri and Enyinnaya, 2022).

A literature survey of the use of natural extract as corrosion inhibitors indicated that the determination of free enthalpy of extract containing various components at different percentages is not adequate. first, because of the use of synergistic of two components, the authors evaluated on the synergistic coefficient to explain a concurrence or cooperative action on the metal surface (Bouklah *et al.*, 2006; Mobin *et al.*, 2013; Kokalj, 2023). In this optic, it's safe to explain the inhibitory effect of the natural extract by the intermolecular synergistic effect via the various active centres containing aromatic rings, double and/or triple bonds as well as heterotaoms reinforcing the adsorption phenomenon on the metal surface (Benali *et al.*, 2013; Mobin *et al.*, 2013; Khadom *et al.*, 2022; Zakeri *et al.*, 2022; Lrhoul *et al.*, 2023).

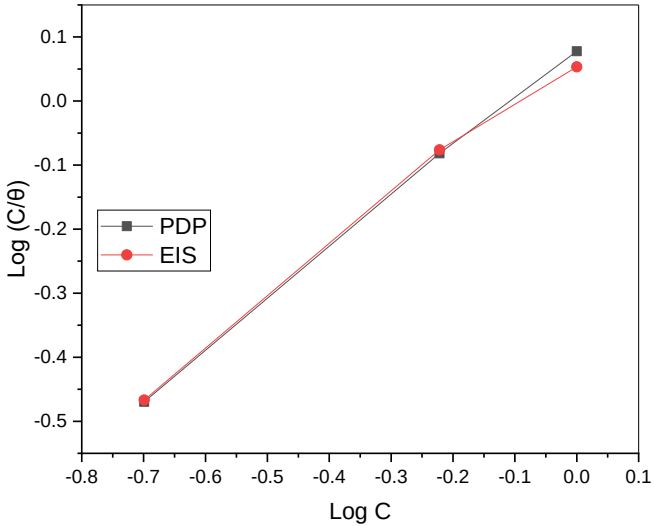

Figure 8: Langmuir Isotherm for adsorption of REUL on Mild Steel surface

Table 5: Langmuir Isotherm Parameters

Electrochemical Technique	**Slope**	**Intercept**	**K_{ads}**	**ΔG_{ads} (kJ/gL^{-1})**	**R^2**
PDP	0.7877	0.08392	0.8243	-9.633	0.998
EIS	0.7559	0.06878	0.8535	-9.721	0.989

Conclusion

Root extract of *Urena lobata* (REUL) is a good suppressor of mild steel deterioration in 0.5 M H_2SO_4. Potentiodynamic polarization (PDP) revealed that REUL is a mixed-type inhibitor reducing both anodic and cathodic corrosion reactions. Electrochemical Impedance Spectroscopy (EIS) showed that REUL functions by forming a protective layer on the mild steel surface, with the charge transfer resistance (R_{ct}) increasing in proportion to the extract concentration. Adsorption of REUL on the mild steel surface followed the Langmuir Isotherm with R^2 values greater than 0.98 for both PDP and EIS. Thermodynamically, the adsorption of REUL onto the mild steel surface is spontaneous as can be seen from the negative ΔG_{ads} values.

Acknowledgement: The authors are grateful to The Academy of Scientific and Innovative Research (AcSIR) CSIR-Central Electrochemical Research Institute (CECRI) Karaikudi-630003, Tamil Nadu, India for using their laboratory and other facilities in this research.

Disclosure statement: *Conflict of Interest:* The authors declare that there are no conflicts of interest.

References

Adil Mahraz M., Salim R., Loukil E.H., Assouguem A., Kara M., *et al*. (2024). Exploratory evaluation supported by experimental and modeling approaches of Inula viscosa root extract as a potent corrosion inhibitor for mild steel in a 1 M HCl solution. *Open Life Sciences*, 19(1), 20220879.

Arrousse N., Salim R., Abdellaoui A., ElHajjaji F., *et al*. (2021), Synthesis, characterization, and evaluation of xanthene derivative as highly effective, nontoxic corrosion inhibitor for mild steel immersed in 1 M HCl solution, *Journal of the Taiwan Institute of Chemical Engineers*, 120, 344-359, https://doi.org/10.1016/j.jtice.2021.03.026

Azgaou, K., Damej, M., El Hajjaji, S., Sebbar, N. K., Elmsellem, H., El Ibrahimi, B., Benmessaoud, M. (2022). Synthesis and characterization of N-(2-aminophenyl)-2-(5-methyl-1H-pyrazol-3-yl) acetamide (AMPA) and its use as a corrosion inhibitor for C38 steel in 1 M HCl. Experimental and theoretical study. *Journal of Molecular Structure*, *1266*, 133451. https:/dx.doi.org/10.1016/j.molstruc.2022.133451

Azzaoui K., Mejdoubi E., Jodeh S., Lamhamdi A., Rodriguez-Castellón E., *et al*. (2017) Eco friendly green inhibitor Gum Arabic (GA) for the corrosion control of mild steel in hydrochloric acid medium, *Corrosion Science* 129, 70-81

Benali O., Benmehdi H., Hasnaoui O., Selles C., Salghi R. (2013). Green corrosion inhibitor: inhibitive action of tannin extract of Chamaerops humilis plant for the corrosion of mild steel in 0.5 M H_2SO_4, *J. Mater Environ. Sci*, 4 (1), pp. 127-138

Bouklah M., Hammouti B., Aouniti A., Benhadda T. (2004), Thiophene derivatives as effective inhibitors for the corrosion of steel in 0.5M H2SO4. *Prop. Org. Coat.* 49N°3, 225-228, https://doi.org/10.1016/j.porgcoat.2003.09.014

Bouklah M., Hammouti B., Aouniti A., Benkaddour M., Bouyanzer A., (2006). Synergistic effect of iodide ions on the corrosion inhibition of steel in 0.5 M H2SO4 by new chalcone derivatives, *Appl. Surf. Sci.* 252N°18, 6236-6242

Chetouani A., Medjahed K., Sid-Lakhdar K.E., *et al*. (2004), Poly(4-vinylpyridine poly(3-oxide ethylene) tosyle) an excellent inhibitor for iron in sulphuric acid medium at 80°C. *Corros. Sci.* 46, 2421-2430, https://doi.org/10.1016/j.corsci.2004.01.020

de Britto Policarpi, E., & Spinelli, A. (2020). Application of *Hymenaea stigonocarpa* fruit shell extract as eco-friendly corrosion inhibitor for steel in sulfuric acid. *Journal of the Taiwan Institute of Chemical Engineers*, *116*, 215-222.

Diki, N. Y. S., Bohoussou, K. V., Kone, M. G. R., Ouedraogo, A., & Trokourey, A. (2018). Cefadroxil drug as corrosion inhibitor for aluminum in 1 M HCl medium: experimental and theoretical studies. *IOSR Journal of Applied Chemistry*, *11*, 24-36.

Di Meo, M. C., Izzo, F., Rocco, M., Zarrelli, A., Mercurio, M., Varricchio, E. (2022). Mid-Infrared spectroscopic characterization: New insights on bioactive molecules of *Olea europaea* L. leaves from selected Italian cultivars. *Infrared Physics & Technology*, 127, 104439.

Elmsellem H., Youssouf M. H., Aouniti A., *et al*. (2014), Adsorption and inhibition effect of curcumin on mild steel corrosion in hydrochloric acid, *Russian J. Appl. Chem.*, 87 (6), 744-753, https://doi.org/10.1134/S1070427214060147

Enyinnaya, N. P., James, A. O., Obi, C. (2021). Corrosion inhibition of *Urena lobata* leaves extract on mild steel corrosion in H_2SO_4 acid. *International Journal of advances in Engineering and Management*, *3*(12), 1275-1286.

Enyinnaya N. P., James A. O., Obi C. (2022). Inhibitive potential of benign Caesar-weed leaves extract (CWLE) as corrosion inhibitor of aluminium in H_2SO_4 phase. *Interdisciplinary Journal of Applied and Basics Subjects*, *2*(1), 1-13.

Enyinnaya, N. P., James, A. O., & Obi, C. (2024). Bark Extract of *Urena lobata* as Green Corrosion Inhibitor for Mild Steel in Sulphuric Acid Environment. *Journal of Material and Environmental Science*, *15*(12), 1776-1795.

Fouda, A. E. A. S., Abd el-Maksoud, S. A., El-Sayed, E. H., Elbaz, H. A., Abousalem, A. S. (2021). Retracted Article: Effectiveness of some novel heterocyclic compounds as corrosion inhibitors for carbon steel in 1 M HCl using practical and theoretical methods. *RSC advances*, *11*(31), 19294-19309.

Fouda, A. E. A. S., Al-Bonayan, A. M., Molouk, A. F., Eissa, M. (2022). Aizoon extract as an eco-friendly corrosion inhibitor for stainless steel 430 in HCl solution. *RSC advances*, *12*(48), 30906-30920.

Gao, X. L., Liao, Y., Wang, J., Liu, X. Y., Zhong, K., Huang, Y. N., Gao, H, Gao B. and Xu, Z. J. (2015). Discovery of a potent anti-yeast triterpenoid saponin, clematoside-S from *Urena lobata* L. *International Journal of Molecular Sciences*, *16*(3), 4731-4743.

Hadisaputra, S., Zulhijayanti, R., Siahaan, J., Savalas, L. R. T., Hamdiani, S., Gapsari, F. (2025). Experimental and Computational Investigation of Spearmint (*Mentha spicata* L.) Extract as a Green Corrosion Inhibitor for Copper in a Sulfuric Acid Environment. *Physical Chemistry Research*, *13*(2), 413-427.

Harvey J.P., Courchesne W., Vo M.D. *et al.* (2022). Greener reactants, renewable energies and environmental impact mitigation strategies in pyrometallurgical processes: A review. *MRS Energy & Sustainability*, 9, 212–247, https://doi.org/10.1557/s43581-022-00042-y

Idouhli, R., Oukhrib, A., Koumya, Y., Abouelfida, A., Benyaich, A., Benharref, A. (2018). Inhibitory effect of *Atlas cedar* essential oil on the corrosion of steel in 1M HCl. *Corrosion Reviews*, *36*(4), 373-384.

Ismail, M. A., Shaban, M. M., Abdel-Latif, E., Abdelhamed, F. H., Migahed, M. A., El-Haddad, M. N., Abousalem, A. S. (2022). Novel cationic aryl bithiophene/terthiophene derivatives as corrosion inhibitors by chemical, electrochemical and surface investigations. *Scientific Reports*, *12*(1), 3192

Islam, M. T., Uddin, M. A. (2017). A revision on *Urena lobata* L. *International Journal of Medicine*, *5*(1), 126-131.

Jasim, E. Q., Mohammed-Ali, M. A., & Hussain, A. A. (2015). Investigation of *Salvadora persica* roots extract as corrosion inhibitor for mild steel in 1 M HCl and in cooling water. *Chemistry and Materials Research*, *7*(4), 147-159.

Jisha, M., Hukuman, N. Z., Leena, P., & Abdussalam, A. K. (2019). Electrochemical, computational and adsorption studies of leaf and floral extracts of *Pogostemon quadrifolius* (Benth.) as corrosion inhibitor for mild steel in hydrochloric acid. *Journal of Material and Environmental Science*, *10*(9), 840-853.

Karra D., Timoudan N., Bazanov D. R., *et al*. (2025). Corrosion inhibition performance of imidazole derivative for protection of carbon steel in hydrochloric acid solution: Experimental and theoretical analysis. *International Journal of Electrochemical Science*, *20*(6), 101015.

Kaya, F., Solmaz, R., & Gecibesler, I. H. (2023). Adsorption and corrosion inhibition capability of Rheum ribes root extract (Işgın) for mild steel protection in acidic medium: A comprehensive electrochemical, surface characterization, synergistic inhibition effect, and stability study. *Journal of Molecular Liquids*, *372*, 121219.

Keke C.O., Nsofor W.N., Kumabia F.K.R., Iloabuchi G.C., Ejiofor J.C., Osuagwu O.L. (2023) GCMS and FTIR analysis of ethanol and methanol leave extract of Urena lobata (Caesar weed) for bioactive phytochemical constituents. *J. Drug Delivery Ther.* ;13(1), 99-115. Available from: https://jddtonline.info/index.php/jddt/article/view/5722

Khadom A. A., Abd, A. N., Ahmed, N. A. (2022). Synergistic effect of iodide ions on the corrosion inhibition of mild steel in 1M HCl by Cardaria Draba leaf extract, *Results in Chemistry,* 4, 100668, ISSN 2211-7156, https://doi.org/10.1016/j.rechem.2022.100668

Khayatkashani, M., Soltani, N., Tavakkoli, N., Nejatian, A., Ebrahimian, J., Mahdi, M. A., & Salavati-Niasari, M. (2022). Insight into the corrosion inhibition of *Biebersteinia multifida* root extract for carbon steel in acidic medium. *Science of the Total Environment*, *836*, 155527.

Kokalj A. (2023). Considering the concept of synergism in corrosion inhibition, *Corrosion Science,* 212,110922, ISSN 0010-938X, https://doi.org/10.1016/j.corsci.2022.110922

Lahmady, S., Anor, O., Forsal, I., Mernari, B., Hanin, H., Benbouya, K., & Talfana, A. (2023). Investigation of *Ziziphus Lotus* Leaves Extract Corrosion Inhibitory Impact on Carbon Steel in a Molar Hydrochloric Acid Solution. *Port. Electrochim. Acta*, *41*, 135-149.

Lrhoul H., Sekkal H. & Hammouti B. (2023) Natural Plants as Corrosion Inhibitors: Thermodynamic's restrictions, *Mor. J. Chem.,* 14(3), 689-698

Mobin M., Alam Khan M. (2013). Investigation on the Adsorption and Corrosion Inhibition Behavior of Gum Acacia and Synergistic Surfactants Additives on Mild Steel in 0.1 M H_2SO_4, *J. Disp. Sci. Technol.*, 34(11), 1496-1506, https://doi.org/10.1080/01932691.2012.751031

Momoh-Yahaya, H., Eddy, N. O., Iyun, J. F., Gimba, C. E., & Oguzie, E. E. (2012). Inhibitive and adsorptive behaviour of guanine on corrosion of mild steel in 0.1 M HCl and H_2SO_4. *International Journal of Modern Chemistry*, *2*(3), 127-142.

Njoku, D. I., Chidiebere, M. A., Oguzie, K. L., Ogukwe, C. E., & Oguzie, E. E. (2013). Corrosion inhibition of mild steel in hydrochloric acid solution by the leaf extract of *Nicotiana tabacum*. *Advances in Materials and Corrosion*, *2*(1), 54-61.

Nzeneri, U. J., Enyinnaya, N. P. (2022). Corrosion of aluminium in hydrochloric acid solution containing thiodiglycolic acid. *Journal of Material and Environmental Science*, *13*(5), 553-563.

Oueslati, K., Nasti, R., Magni, M., Trasatti, S., Amor, Y. B. (2025). Glaucium Extract as an Effective Green Corrosion Inhibitor for Mild Steel in High Concentrated Sulfuric Acid Solution. *Chemistry Select*, *10*(21), e00514.

Pal, A., Das, C. (2022). Investigations on corrosion inhibition in acidic media for BQ steel using banana flower bract, an eco-friendly novel agro-waste: Experimental and theoretical considerations. *Inorganic Chemistry Communications*, *145*, 110024.

Rahmouni, H., Nigri, S., Oumeddour, R., Guendouzi, A., Berkane, A., Nacef, M., Affoune, A. M. (2025). Experimental and theoretical investigations into green approach steel corrosion inhibition performance of an aqueous mixture of *Olea europaea* and *Ficus carica* leaves extract in acid medium. *RSC advances*, *15*(26), 20355-20371.

Saha, S. K., and Kang, N. (2022). Corrosion: basics, economic adverse effects, and its mitigation. *Carbon Allotropes: Nanostructured Anti-Corrosive Materials*, 67.

Sanaei, Z., Ramezanzadeh, M., Bahlakeh, G., & Ramezanzadeh, B. (2019). Use of *Rosa canina* fruit extract as a green corrosion inhibitor for mild steel in 1 M HCl solution: A complementary

experimental, molecular dynamics and quantum mechanics investigation. *Journal of Industrial and Engineering Chemistry*, *69*, 18-31. https://doi.org/10.1016/j.jiec.2018.09.013

Shathani, P., Ogunmuyiwa, E. N., Oladijo, O. P., & Obadele, B. A. (2025). Thermodynamics and adsorption behaviour of *Sclerocarya birrea* leaf extract as a potential green corrosion inhibitor for mild steel in a simulated seawater (3.5% NaCl) environment. *Chemical Thermodynamics and Thermal Analysis*, 100197.

Singare, S., Jain, N. K., Upadhyay, P., & Tomar, V. S. (2022). Antiulcer Potential of Extracts of Urena lobata Plant Leaves. *International Journal of Medical Sciences and Pharma Research*, 8(3), 8–13. https://doi.org/10.22270/ijmspr.v8i3.48

Song, H., Yasin, G., Singh, N. B., Gupta, R. K., & Nguyen, T. A. (Eds.). (2022). *Nanotechnology in the automotive industry*. Elsevier.Pages 371-401 Nanotechnology in the Automotive Industry, 2022

Thakur, A., Dagdag, O., Berisha, A. *et al.*, (2024) Experimental accompanied with computational (atomic/electronic)-level simulation investigations of *Polygonum cuspidatum* root extract as sustainable corrosion inhibitor for mild steel in aggressive corrosive media. *Environ Sci Pollut Res*. https://doi.org/10.1007/s11356-024-34141-9

Udom, I. G., Cookey, G. A., Ameh, P. O. (2025) Investigation of *Acanthus montanus* Leaves Extract as Corrosion Inhibitor for Copper in 2 M Sulphuric Acid. *Communication in Physical Sciences*, 12(3) 778-798. https://dx.doi.org/10.4314/cps.v12i3.9

Zakeri A., Bahmani E., Aghdam ASR. (2022), Plant extracts as sustainable and green corrosion inhibitors for protection of ferrous metals in corrosive media: A mini review, *Corrosion Communications*, 5, 25-38, ISSN 2667-2669, https://doi.org/10.1016/j.corcom.2022.03.002

Žbulj, K., Hrnčević, L., Bilić, G., Simon, K. (2022). Dandelion - root extract as green corrosion inhibitor for carbon steel in CO_2 - saturated brine solution. *Energies*, *15*(9), 3074.

Zomorodian, A., Garcia, M. P., e Silva, T. M., Fernandes, J. C. S., Fernandes, M. H., Montemor, M. D. F. (2015). Biofunctional composite coating architectures based on polycaprolactone and nanohydroxyapatite for controlled corrosion activity and enhanced biocompatibility of magnesium AZ31 alloy. *Materials Science and Engineering: C*, *48*, 434-443.